Chemical Engineering Journal 97 (2004) 87–101

Chemical Engineering Journal

www.elsevier.com/locate/cej

Optimal control of product quality for batch nylon-6,6 autoclaves

Marcel Joly [a], José M. Pinto [a,b,*]

[a] *Department of Chemical Engineering, University of São Paulo, São Paulo SP 05508-900, Brazil*
[b] *Department of Chemical Engineering and Chemistry, Polytechnic University, Brooklyn, NY 11201, USA*

Received 29 November 2002; accepted 29 April 2003

Abstract

Dynamic optimization problems are usually solved by transforming them into nonlinear programming (NLP) models with either sequential or simultaneous approaches. In this paper, the potential and limitations of both procedures in solving a general batch nylon-6,6 autoclave optimization model are evaluated and discussed. Nylon-6,6 is a highly value-added good produced in large-scale under many different specifications. Highly nonlinear behavior, lack of on-line measurements of polymer qualities and several disturbances inherent to this process motivate its optimal operation. In addition, the operation during the finishing stage of the batch polycondensation is crucial since it largely determines the final product molecular weight and quality. Results show that both strategies can be successfully applied to solve the dynamic optimization problem only after an expressive level of investments in terms of modeling implementation. However, the simultaneous strategy has the advantage that specification constraints can be directly enforced in the model, thus generating better and more robust results.

Keywords: Optimal control; Nylon-6,6; Nonlinear programming; Optimization

1. Introduction

1.1. Preliminaries

Due to the ever-increasing global competition environment, several factors have encouraged better monitoring and control strategies of end-use quality variables in nylon-6,6 polymerization processes. Nylon-6,6 is a highly value-added good produced in large-scale under many different specifications. Moreover, it is well-known that process operation play an important role in both reactor design and control. In particular, the highly nonlinear behavior of the process, the frequent obstacles in on-line reactor measurements of nylon-6,6 end-use qualities as well as the several disturbances inherent to this process (e.g., water content in the feed) have emphasized the importance of reactor modeling. Furthermore, this problem is often embedded in higher-level problems, as the plant-wide dynamic optimization aiming to produce optimally integrated planning and scheduling policies, whose benefits are well documented in other fields of chemical engineering [1], given the important ease that relatively sophisticated plant-wide dynamic models involving thousands of states can now be handled through the existing technology.

On the other hand, limited up to the middle of the 1980s not only by computational restrictions but decisively due to little availability of published information, detailed simulation and optimization of nylon-6,6 reactors had to be postponed to the 1990s. Till then, kinetic information was practically reduced to the pioneers, nevertheless limited results from Ogata [2,3]. Additionally, there was no published data on vapor–liquid equilibrium to model water vaporization. This information is very crucial since the final degree of polymerization depends on the water concentration in the melt, and this in turn depends on the pressure and temperature, as well as the composition of the liquid phase.

As a consequence of subsequent studies about kinetic modeling produced ever since [4,5], the recent years have been characterized by an increasing number of modeling developments and refinements reported in the open literature that addresses nylon-6,6 production in a number of different reactors. Thin or continuous wiped film reactors modeling have been studied by Steppan et al. [6] and Choi and Lee [7]. Giudici et al. [8] addressed the catalytic and homogeneous process conduced in twin-screw extruder reactors. Batch autoclave models and control strategies have been investigated by Russell et al. [9], whereas practical approaches to the control of final product quality in semi-batch reactors are discussed by Yabuki et al. [10] and Clarke-Pringle and MacGregor [11]. Tubular reactors under two-phase flow conditions without external catalyst are

* Corresponding author. Tel.: +1-718-260-3569; fax: +1-718-260-3125.
E-mail address: jpinto@poly.edu (J.M. Pinto).

1385-8947/$ – see front matter © 2003 Elsevier B.V. All rights reserved.
doi:10.1016/S1385-8947(03)00132-3

Nomenclature

C_i	concentration of i (mol/l)
C_p	specific heat capacity of the liquid phase (cal/(g °C))
C_T	total concentration (mol/l)
E_{app}	activation energy for degradation reaction j (cal/mol)
E_{kapp}	apparent activation energy (cal/mol)
ΔH_{app}	apparent enthalpy of reaction (cal/mol)
ΔH_v^i	heat of vaporization of i (cal/mol)
k_{app}	apparent forward reaction constant (mol/total mol h)
k_j	kinetic constant for degradation reaction j (mol/total mol h)
k_0	reference apparent forward rate constant (mol/total mol h)
k_{0j}	reference forward rate constant for degradation reaction j (mol/total mol h)
k_{0j}	kinetic constant rate for degradation reaction j (h^{-1})
K	overall mass transfer coefficient (g/(h psia))
K_{app}	apparent equilibrium constant for polycondensation reaction (dimensionless)
K_0	reference apparent equilibrium constant (dimensionless)
M_i	molecular weight of i
M_{ii}	molecular weight of a i–i segment within the polymer molecule
M_0	molecular weight of one unit of the polymer chain
MW	average molecular weight of the polymer
n_w	moles of water/mole of fundamental unit (l)
n_1	fraction of polymer molecules that are HMD
NH_2	amine end concentration (mol/g)
P	reactor pressure (psia)
P^{vap}	solution vapor pressure (psia)
P_i^{sat}	pure component vapor pressure (psia)
Q_{heat}	heat input (cal/h)
r	stoichiometric ratio of monomers
R	gas constant
R_j	rate of reaction j (mol/(l h))
T	reactor temperature (K)
T_0	reference temperature (K)
T_{0j}	reference temperature for degradation reaction j (K)
v	vent flow rate (g/h)
v_i^M	molar rates of vaporization of i (mol/h)
V	volume of liquid phase (l)
$\hat{V}$	specific volume (l/kg)
x_i	mole fraction of i in the liquid phase
y_i	mole fraction of i in the vapor phase

Greek letters

ε	extent of reaction
μ_i	mass fraction of i in the liquid phase
ρ	liquid phase density (g/l)
ω_i^e	mass fraction of i in the vapor phase

Subscripts

A	amine end groups
C	carboxylic end groups
HMD	hexamethylene diamine monomer
i	components A, C, HMD, L, SE and W
j	reactions
L	polymer link
SE	stabilized end groups
W	water molecule

reported by Giudici et al. [12]. Concomitantly, these models, which in most part rely on (strongly) nonlinear systems of differential-algebraic equations (DAEs), have motivated the study and development of solution techniques.

Following this trend, while alternative optimization approaches, as neural networks (NN) or multi-way projection to latent structures (MPLS) are living important developments [13,14], nonlinear programming (NLP) under constraints remains as basis of major solution techniques currently used by schedulers [1]. Nevertheless, NLP optimization technology still requires ability to deal with some well-known algorithmic limitations. As pointed out in [13], NLP gradient-based approaches usually have to cope with problems such as numerical evaluations of derivatives (Jacobians and Hessians) and feasibility issues [15]. Moreover, conventional use of decomposition schemes for dynamic systems implies in additional difficulties associated with the resulting NLP, as the presence of algebraic equations (the index problem), the high dimensionality of discretized problems, the solution of state equations specially with unstable components and the definition of the finite element lengths for discretization [16].

On the other hand, derivative-free (or direct search) methods usually overcome some of these drawbacks, so they may offer a practical approach given the current state of technology. However, the main deficiency of direct search comes from the fact that the nonlinear model, which is normally a time-consuming task, must be solved at each algorithm iteration. Furthermore, the existence of local solutions in optimization problems is frequent, that may be partially circumvented by running the optimization algorithm several times with different starting points for decision variables.

The contribution of this research is twofold. Firstly, two general and comprehensive NLP-based methodologies for

optimal control of a generic batch nylon-6,6 autoclave model are proposed in order to provide useful tools for defining operating profiles, which can perform as set-point programs for control systems. Second, the computational performance of the two approaches are compared and discussed in terms of algorithmic structures and solution methods.

As basis for the proposed work, we have selected the fundamental process model presented in [9], since it captures the dominant features of the process behavior. In order to provide a better understanding of the problem, the next subsections take a more in-depth view at the inherent features of the nylon-6,6 polymerization chemistry as well as at the batch nylon-6,6 autoclave process. The fundamental model is introduced in Section 2. Section 3 outlines the mathematical background of the approaches used to solve the previous differential-algebraic optimization problem (DAOP). Model simulation, optimization results and evaluation of the solution techniques are presented in Section 4. Section 5 concludes the paper and summarizes future directions.

1.2. The chemistry of nylon-6,6 polymerization

Nylon-6,6 or poly(hexamethylene adipamide) is usually synthesized in a multistage process in which the product is obtained from thermal decomposition of nylon-6,6 salt (hexamethylene diammonium adipate). As will be discussed in the next subsection, this salt has the advantage of presenting an exact 1:1 stoichiometric ratio between $–NH_2$ and –COOH groups. Although nylon-6,6 production may be carried on quite a number of different ways from an engineering standpoint, the chemistry involved is essentially the same.

This paper is concerned with the production of nylon-6,6 by direct amidation of adipic acid and hexamethylene diamine in a batch process carried out in autoclave reactors (Fig. 1). In this process, the reactor feed is composed by molten adipic acid and hexamethylene diamine in approximately stoichiometric proportions. The polyamidation can be treated as a second-order reversible reaction of the a–a/b–b type commonly described in terms of functional groups for the sake of simplicity. The overall reaction model for the nylon-6,6 batch autoclave is shown in Table 1, where A is an amine end group ($–NH_2$), C is a carboxyl end group (–COOH), W is a water molecule, L is a polymer link (–CONH–) and SE refers to a cyclic or stabilized end group.

Table 1
Nylon-6,6 reaction model [9]

Degradation	$C \rightarrow SE + W$	(1)
	$L \rightarrow SE + A$	(2)
Polyamidation	$A + C \leftrightarrow L + W$	(3)

1.3. Overview of the process

In short, amine end groups on either HMD or polymer chain react with carboxylic end groups on either adipic acid monomer or polymer chain, according to Eq. (3), to form a polymer chain link and a molecule of water. Also, degradation reactions (Eqs. (1) and (2)) must be considered [6] since they affect the temperature dependence of the resulting average molecular weight of the polymer (MW). Some authors [12] also consider a more complete model by adding the degradation of SE (into CO_2 and a Schiff base) to the model in Table 1. However, we neglect that reaction, as in [9], in benefit of a simpler formulation.

In most cases, the industrial objective is to maximize productivity regarding the required end-use product quality. Eventually, other objectives should be considered due to the need of blending with some off-spec product or even when batch time does not need to be minimized. The end-use product quality is defined by the MW level and the amine end concentration (NH_2). In this paper, we are concerned with maximizing nylon-6,6 production under product specifications for constrained batch run times. In order to achieve the desired end-use product quality, the extent of reaction must be above 99%. Therefore, the equilibrium is shifted towards completion by continuous vaporization of water (see Eq. (3)). Another complicating factor is that MW is very sensitive to the stoichiometric feed ratio (r) of monomers A and C, which must be kept near unity. It is worth to note that since A is supplied by HMD (two A per HMD), which is also volatile, the loss of HMD through vaporization (and the subsequent deviation of r from unity) represents an important drawback to this approach [9]. Vaporization requirement is satisfied by an autoclave reactor (Fig. 2) where there

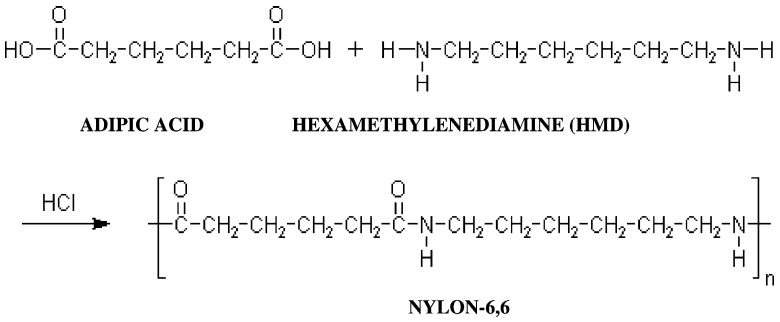

Fig. 1. Nylon-6,6 reaction.

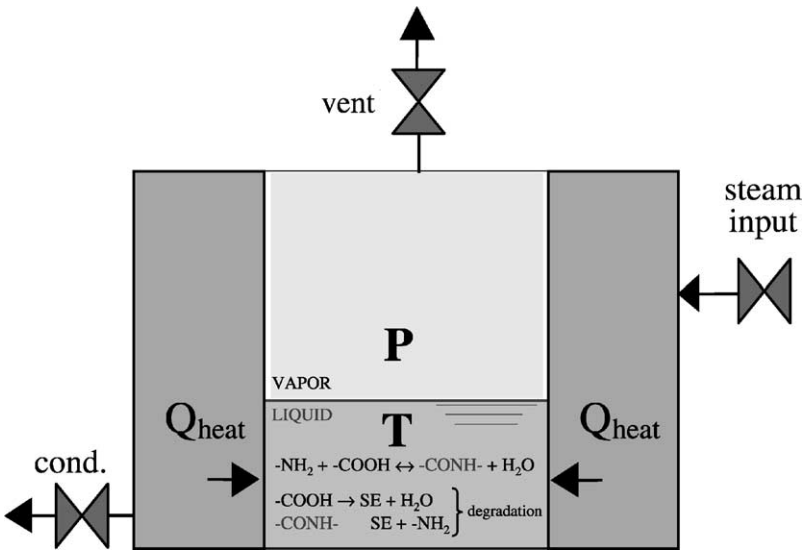

Fig. 2. Schematic representation of the batch nylon-6,6 autoclave.

is a valve for venting vaporized water and a steam jacket that also supplies heat to the reaction medium.

During the batch operation, product quality is usually monitored by on-line measurements of secondary process variables, since MW and NH_2 can be solely measured after the batch run. Typically, these measurements include readings of the reactor pressure (P), steam jacket pressure, vent flow rate and temperature of the liquid phase (T). The reactor operation can be suitably divided into three distinct stages [9]. In the first one, the *initial heating phase*, an aqueous equimolar mixture of HMD and adipic acid is charged to the autoclave that has been previously purged of oxygen. An extra amount of HMD can also be added in order to compensate losses of this reactant by vaporization. Once charging is concluded, the exothermic salt formation provides an important amount of the necessary heat to raise the batch temperature and complementary heat is supplied to the system by the steam jacket to force the polymerization reaction to begin. At this stage, the reactants are not yet well-mixed and the pressure above the reacting solution is maintained higher than the vapor pressure of the liquid phase to avoid premature loss of volatile amine feed monomer HMD. Therefore, since the vent valve is kept closed during this initial phase, the ratio r remains constant. When a sufficient rate of polymerization in terms of reacted HMD is achieved, the vent valve is then opened to allow the escape of vaporized water. The valve opening starts the *boiling phase*, in which water is continuously vented off the reactor with the objective of allowing high MW polymer levels. Furthermore, mass transport in the liquid phase becomes more effective due to boiling and a well-mixed medium is obtained. The *finishing phase* starts when water has been removed and boiling no longer occurs. This important stage of the nylon-6,6 process has been extensively studied [6,17] since it sets the quality of the final product. In his phase, heat addition is complicated not only by the increased viscosity in the medium due to the high polymer MW, but also by reactor fouling. Also, because of the high polymer melt viscosity during the latter stages of polymerization, the rate of water removal becomes a critical factor for the polymerization extent. Therefore, some measures are frequently taken to facilitate removal of water, as inert gas bubbling through the melt, increase of agitation rate or application of partial vacuum. Ultimately, the desired end-use product quality should normally be met under time limitations in order to reduce degradation effects.

2. Fundamental model

As a basis for the proposed study, the fundamental nylon-6,6 batch autoclave model from Russell et al. [9] is selected since it incorporates a comprehensive and well-known phenomenological structure supported by first-principles along with some empirical relations that are tailored for the system. Moreover, the model is complete with respect to all complementary information (kinetic and physical properties). In short, the model relies on the following major assumptions [9]:

(a) thermal effects of the side reactions (Eqs. (1) and (2)) are neglected;
(b) thermal effects of the vapor phase are neglected;
(c) spatial variations are neglected;
(d) the vapor phase molar balance is neglected;
(e) P (reactor pressure) is a manipulated variable;
(f) water and HMD leave the liquid phase according to their vapor–liquid equilibrium relations;
(g) *equal reactivity* (i.e., the reaction rate does not depend on molecular size);
(h) saturated steam is fed into the reactor jacket and heat losses are negligible.

Table 2
The batch nylon-6,6 autoclave model—kinetics [9]

Reaction	Kinetics
Degradation	
$C \rightarrow SE + W$	$R_1 = k_1 C_C$
$L \rightarrow SE + A$	$R_2 = C_L \left(k_2 + k_{2c}\left(\frac{C_A}{C_T}\right)\right)$
Polymerization	
$A + C \leftrightarrow L + W$	$R_3 = \left(\frac{k_{app}}{C_T}\right)\left(C_A C_C - \left(\frac{C_L C_W}{K_{app}}\right)\right)$
Kinetic relations[a]	
$k_i = k_{0_i} \exp\left\{\left(-\frac{E_{app}}{R}\right)\left[\left(\frac{1}{T}\right) - \left(\frac{1}{T_{0_i}}\right)\right]\right\}$, where $E_{app} = 30\,\text{kcal/mol}$, $R = 1.99\,\text{cal/mol K}$	
$K_{app} = K_0 \exp\left\{-\left(\frac{\Delta H_{app}}{R}\right)\left[\left(\frac{1}{T}\right) - \left(\frac{1}{T_0}\right)\right]\right\}$, where $T_0 = 473.15\,\text{K}$, $R = 1.99\,\text{cal/mol K}$	
$K_0 = \exp\left\{\left[1 - 0.47\exp\left(-\frac{\sqrt{x_W}}{0.2}\right)\right](8.45 - 4.2x_W)\right\}$	
$\Delta H_{app} = 7650\tanh[6.5(x_W - 0.52)] + 6500\exp\left(-\frac{x_W}{0.065}\right) - 800$	
$k_{app} = k_0 \exp\left\{\left(-\frac{E_{kapp}}{R}\right)\left[\left(\frac{1}{T} - \frac{1}{T_0}\right)\right]\right\}$, where $T_0 = 473.15\,\text{K}$, $R = 1.99\,\text{cal/mol K}$, $E_{kapp} = 21.4\,\text{kcal/mol}$	
$k_0 = \exp\{2.55 - 0.45\tanh[25(x_W - 0.55)] + 8.58(\tanh[50(x_W - 0.1)] - 1)(1 - 30.05x_C)\}$, where $C_T = C_A + C_C + C_L + C_W + C_{SE}$, $C_{HMD} = 0.5n_1(C_A + C_C + C_{SE})$, $x_W = C_W/C_T$, $x_C = C_C/C_T$, $x_L = C_L/C_T$, $x_{HMD} = C_{HMD}/C_T$	

[a] For rate constant—k_1, k_{0_i}: $0.06\,\text{h}^{-1}$, T_{0_i}: 566 K; k_2, k_{0_i}: $0.005\,\text{h}^{-1}$, T_{0_i}: 578 K; k_{2c}, k_{0_i}: $0.32\,\text{h}^{-1}$, T_{0_i}: 578 K.

Assumption (a) comes from the fact that side reaction rates are much lower than that of the polymerization reaction. Due to the small mass of the vapor phase and its fast dynamics, (b) takes place. Since only the overall reactor pressure in the vapor phase, P, affects the liquid phase dynamics, (d) holds and (e) emerges from the fact that the pressure control loop is fast (i.e., has negligible dynamics) and is sufficiently accurate. In order to describe the molecular size distribution in terms of the Flory distribution [18], (g) is postulated. Finally, from (h) the heat input to the reactor, Q_{heat}, becomes simply the heat given up by the condensing steam and, as a consequence, the manipulation of the jacket pressure, P_j, is fairly simple, provided that condensate flow rate is measurable.

The model is characterized by a set of DAEs and nonlinear expressions for constitutive equations, and are summarized in Tables 2–6. Original references on the kinetics and physical property calculations as well as specific features of the modeling may be found in [9].

As part of the overall formulation, the mass transfer model (Table 3) involves the vapor pressure term (P^{vap}) given as the maximum between P_1^{vap} and P_2^{vap}. While P_2^{vap} relies on

Table 3
The batch nylon-6,6 autoclave model—mass and energy model [9]

Mass and energy balances	Mass transfer model
$\frac{dV C_A}{dt} = VR_2 - (VR_3 + v_A^M)$	$\begin{cases} v = K(P^{vap} - P) & \text{if } P^{vap} > P \\ v = 0 & \text{otherwise} \end{cases}$, $K = 25\,000\,\text{g/(h psia)}$
$\frac{dV C_C}{dt} = -V(R_3 + R_1)$	$v_i^M = \frac{\omega_i^e}{M_i} v, \quad i = \text{W, HMD}$
$\frac{dV C_L}{dt} = V(R_3 - R_2)$	$v_A^M = 2v_{HMD}^M$
$\frac{dV C_W}{dt} = V(R_3 + R_1) - v_w^M$	*Vapor–liquid equilibrium (VLE) relations*
$\frac{dV C_{SE}}{dt} = V(R_1 + R_2)$ and $\frac{d\rho V}{dt} = -v$	$\frac{y_{HMD}}{y_W} = \alpha\frac{x_{HMD}}{x_W}$, where $\alpha = \frac{P_{HMD}^{sat}}{P_W^{sat}}$
$\frac{dT}{dt} = -\frac{\Delta H_p R_3}{\rho C_p} - \frac{\Delta H_v^{HMD} v_{HMD}^M}{\rho C_p V} - \frac{\Delta H_v^W v_W^M}{\rho C_p V} + \frac{Q_{heat}}{\rho C_p V}$ with $\Delta H_v^W = \frac{7.724T^2}{(T - 45.15)^2}$, $\Delta H_v^{HMD} = 12.4\,\text{kcal/mol}$; T in K	

Table 4
The batch nylon-6,6 autoclave model—quality variables [9]

$$\mathrm{MW} = \frac{M_0(1+r)}{1+r-2\varepsilon} \quad \text{and} \quad \mathrm{NH_2} = \frac{10^6 C_\mathrm{A}}{\rho} \quad \text{with} \quad M_0 = \frac{M_{\mathrm{AA}}\left\{(VC_\mathrm{A})_0 - \int_0^t (2\omega^\mathrm{e}_\mathrm{HMD} v/M_\mathrm{HMD})\,\mathrm{d}t\right\} + M_{\mathrm{CC}}(VC_\mathrm{C})_0}{(VC_\mathrm{A})_0 - \int_0^t (2\omega^\mathrm{e}_\mathrm{HMD} v/M_\mathrm{HMD})\,\mathrm{d}t + (VC_\mathrm{C})_0}$$

Table 5
The batch nylon-6,6 autoclave model—physical properties [9]

Physical properties
Specific volumes (V's in l/kg and T in K)
$\hat{V}_\mathrm{W} = (1.0046715 - 1.99824\times10^{-4}[T-273.15] - 2.6321\times10^{-6}[T-273.15]^2)^{-1}$
$\hat{V}_\mathrm{poly} = (1.13 - 0.00052[T-273.15])^{-1}$
$\hat{V}_\mathrm{sol} = \hat{V}_\mathrm{W}[\mu_\mathrm{W} + 0.925(1-\mu_\mathrm{W}-\mu_\mathrm{L})] + \hat{V}_\mathrm{poly}\mu_\mathrm{L}$
Vapor pressure relations (P's in psia and T in K)
$P^\mathrm{sat}_\mathrm{HMD} = \exp[-1.164316 + 6237.44(0.002807 - T^{-1})]$ $\log_{10}\left(\frac{760P^\mathrm{sat}_\mathrm{W}}{14.7}\right) = -\left(\frac{1668.21}{T-45.15}\right) + 7.96681$
$P^\mathrm{vap} = \max(P^\mathrm{vap}_1, P^\mathrm{vap}_2)$, where $\log_{10}\left(\frac{n_\mathrm{W}}{760P^\mathrm{vap}_1/14.7}\right) = \left(\frac{3050}{T}\right) - 10.09$, $P^\mathrm{vap}_2 = x_\mathrm{W}P^\mathrm{sat}_\mathrm{W} + x_\mathrm{HMD}P^\mathrm{sat}_\mathrm{HMD}$
Specific heat capacities (C_p in cal/(g °C) and T in K)
$C_{pw} = 0.997092 + 3.96106\times10^{-5}(T-273.15) - 5.4726\times10^{-7}(T-273.15)^2 + 1.2037\times10^{-8}(T-273.15)^3$
$C_p = \mu_\mathrm{W}C_{pw} + (1-\mu_\mathrm{W})[0.4\varepsilon^2 + 0.5(1-\varepsilon^2)]$

hypothetical ideality condition for the liquid phase during most part of the process, P^vap_1 corresponds to the Henry's law behavior of the solution for water content not greater than 0.1 wt.% [2]. The calculation of P^vap_1 involves n_w that is given by $C_\mathrm{W}/C_\mathrm{L}$. The mass fraction of water and HMD in the vapor phase, $\omega^\mathrm{e}_\mathrm{W}$ and $\omega^\mathrm{e}_\mathrm{HMD}$, respectively, are obtained through VLE relations. However, the mass balances were postulated in terms of total number of A amine end groups in such mode that it is not possible to distinguish between amine end groups at the extreme of HMD molecules and those at the extreme of polymer molecules [9]. This apparent difficulty is circumvented by assumption (g), which combined with a suitable modification in Flory's molecular weight distribution relations (outlined below) proposed in [9], result in an expression for the HMD concentration, C_HMD (see Table 2), in which the term in parenthesis denotes the total number of polymer molecules and parameter n_1 denotes the fraction of polymer molecules that are HMD.

Also based on the modified Flory's molecular weight distribution model for a–a/b–b polymerization [18], the quality variables are expressed as functions of the modeled process states and their respective initial feed conditions. In short, the modified approach accounts for the fact that HMD is being removed through vaporization whereas C is subject to degradation by forming stabilized end groups that can no longer react (Eqs. (1) and (2)). To overcome these effects that are unaccounted for in Flory's original derivation, Russell et al. [9] consider the amount of HMD that has left the reactor as if it has never been there by assuming that the forward/backward reactions occur fast enough to allow the distribution to reach its new value instantaneously. In this sense, the integral term accounts for the total amount of vaporized HMD. Indeed, since the limiting group for the polymerization reaction may change from C towards A during the process as a consequence of the HMD vaporization, two sets of equations must be properly considered, as shown in Table 6.

Table 6
Modified molecular weight distribution model [9]

Limiting group C ($r < 1$)	Limiting group A ($r > 1$)
$n_1 = \frac{(1-r\varepsilon)^2}{r+1-2r\varepsilon}$	$n_1 = \frac{r(1-\varepsilon)^2}{r+1-2r\varepsilon}$
$\varepsilon = \frac{(VC_\mathrm{C})_0 - VC_\mathrm{C} - VC_\mathrm{SE}}{(VC_\mathrm{C})_0}$	$\varepsilon = \frac{(VC_\mathrm{A})_0 - VC_\mathrm{A} - \int_0^t (2\omega^\mathrm{e}_\mathrm{HMD} v/M_\mathrm{HMD})\,\mathrm{d}t}{(VC_\mathrm{A})_0 - \int_0^t (2\omega^\mathrm{e}_\mathrm{HMD} v/M_\mathrm{HMD})\,\mathrm{d}t}$
$r = \frac{(VC_\mathrm{C})_0}{(VC_\mathrm{A})_0 - \int_0^t (2\omega^\mathrm{e}_\mathrm{HMD} v/M_\mathrm{HMD})\,\mathrm{d}t}$	$r = \frac{(VC_\mathrm{A})_0 - \int_0^t (2\omega^\mathrm{e}_\mathrm{HMD} v/M_\mathrm{HMD})\,\mathrm{d}t}{(VC_\mathrm{C})_0}$

3. Solution strategies

3.1. Numerical solution of dynamic optimization problems

A brief overview of general-purpose methods for the numerical solution of the DAOPs that include a system of ordinary differential equations (ODEs) follows. For convenience, the process model previously introduced is generically posed as an initial value ODE model as in Eq. (4):

$$\begin{aligned} \underset{x,U(t),Z(t)}{\text{Min}} \quad & \phi[x, U(t), Z(t)] \\ \text{s.t.} \quad & c[x, U(t), Z(t)] = 0, \\ & \dot{Z}(t) = F[x, U(t), Z(t), t] \ \ \forall t \in [0, t_f], \\ & Z(0) = Z_0, \quad x^{\mathrm{L}} \le x \le x^{\mathrm{U}}, \\ & U^{\mathrm{L}} \le U(t) \le U^{\mathrm{U}}, \quad Z^{\mathrm{L}} \le Z(t) \le Z^{\mathrm{U}} \end{aligned} \tag{4}$$

where ϕ is the objective function, c the design equality constraint vector, x the time-invariant decision variable vector, t the time, $Z(t)$ ($U(t)$) the state (control) profile vector, x^{L}, x^{U} the decision variable bounds, Z^{L}, Z^{U} (U^{L}, U^{U}) the state (control) profile bounds.

There is an extensive literature on numerical strategies that address such class of problems, which fall on three categories: *dynamic programming* based approaches, *indirect* and *direct* methods. See [19] for review. In short, the *dynamic programming* method was first described by Bellman [20] and was extended to include constraints on the state and control variables by Luus [21]. Indeed, the first attempt to solve the optimal control problem employed concept of the calculus of variations introduced in the 1960s [22]. In this variational approach, the optimization problem is transformed into a two-point boundary value problem (TPBVP) with DAEs. This approach constitutes the basic idea of the *indirect methods* and performs very well for unconstrained problems, but the solution of the TPBVP remains difficult, especially with the addition of profile inequalities in the problem [16].

This paper is concerned with the third class. Since the decision variables of the nylon-6,6 process model can be identified as continuous time-invariant, it is possible to accomplish the optimization by applying variable parameterization approaches, or *direct methods*. In summary, direct methods aim to transform the infinite-dimensional dynamic optimization problem into a finite-dimensional NLP. Within this class, two general approaches, namely *sequential* or control parameterization strategy [23] and *simultaneous* or collocation strategy [24], have been continuously developed and refined [15,16,25–28]. In this paper, we have implemented both strategies as discussed next.

3.2. Sequential strategy

In this approach, the key idea is to discretize the control profiles into piecewise polynomials on finite elements. In an inner loop, the state and sensitivity equations are integrated in an initial value problem (IVP) for fixed control profiles using standard DAE solvers, and this yields function and gradient values for the NLP solver. An optimization routine is then applied to solve a master NLP in an outer loop to update the control actions. Fig. 3 summarizes the method. In this figure, the control $U(t)$ is approximated as piecewise

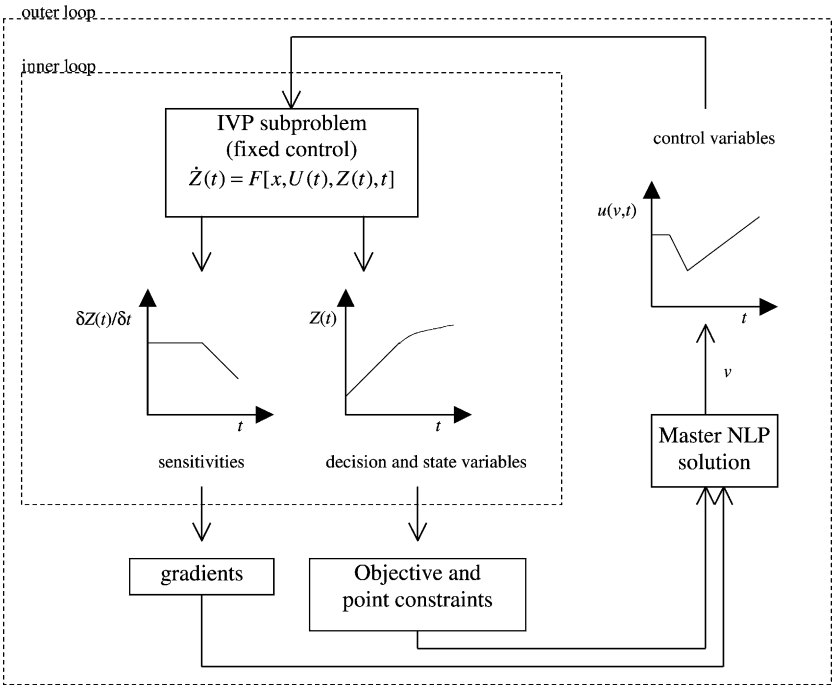

Fig. 3. Scheme of the control parameterization approach to the model (4).

linear functions (hence the term control parameterization), where, in the general case, the slopes, intercepts and extensions of each finite element can be taken as optimization variables in the master NLP.

The major advantage of this strategy lies in the reduced dimensionality of the NLP, since the number of control variables u and parameters remains small even for very complex models. However, inequality constraints and/or boundary conditions on state variables, as the nylon-6,6 quality specifications, cannot be directly enforced [25]. In addition, the solution of the IVP might be infeasible or too costly to converge at intermediate trial points [16].

Discretization using control parameterization allows objective function and point constraints of (4) to be expressed as functions of a finite number of time-invariant variables v (or parameters), which characterize the basis functions. This approach leads to a decomposition of the original DAOP into two subproblems, in which the constraints may in principle be handled in a number of ways [29]. In this paper, we use piecewise linear control policy under N equal sampling intervals, with the requirement for continuity of the control from one finite element to another. Excluding bounds on profiles, the fundamental process model synthesized in (4) does not contain any inequality path constraint, but a number of equality path constraints, which can be included into the DAE model to be solved simultaneously [29]. The targets for the product qualities, which constitute the major state constraints of the problem are imposed as equality point constraints. Based on results from the integration step, these constraints are evaluated at the outer loop and the measured violations are taken into account through penalization of objective in the master NLP. Therefore, the resulting sequential procedure consists of the following steps:

(a) An IVP subproblem, which is the numerical integration of the DAE system formed by $\dot{Z}(t)$ and c for the fixed control $y^{\mathrm{T}} = [x^{\mathrm{T}}, u_1^{\mathrm{T}}(v,t), u_2^{\mathrm{T}}(v,t), \ldots, u_N^{\mathrm{T}}(v,t)]$ determined by the optimization step (or by the initial guess at the first iteration) using the initial state condition of (4). This step yields $z(y)$.

(b) A master NLP subproblem in terms of y, for which the bounds are determined directly from (4):

$$\begin{aligned} \underset{v}{\mathrm{Min}} \quad & \phi[z(y), y] + \omega\, \mathrm{err}_{\mathrm{MW}}^{\gamma}\, \mathrm{err}_{\mathrm{NH_2}}^{\eta} \\ \text{s.t.} \quad & Z_q^{\mathrm{target}} - Z_q = \mathrm{err}_q \quad q = \mathrm{MW}, \mathrm{NH_2}, \\ & y^{\mathrm{L}} \le y \le y^{\mathrm{U}} \end{aligned} \tag{5}$$

As seen, we have included the term $\omega\, \mathrm{err}_{\mathrm{MW}}^{\gamma}\, \mathrm{err}_{\mathrm{NH_2}}^{\eta}$ to the original objective of (4) to account for deviations from the product qualities targets in (5). Here, ω is a weighting factor and γ and η are real exponents. In principle, the master NLP can be solved with either gradient-based approaches such as generalized reduced gradient (GRG) [30] or successive quadratic programming (SQP) [31], or gradient-free approaches such as direct search or stochastic search [32,33]. Nevertheless, efficient control parameterization usually requires the gradients of the objective function and constraints with respect to the optimization parameters [19]. This in turn justifies in part the extensive work that has been produced in order to evaluate the sensitivities in mathematical programming [34]. Reviews on both theoretical and computational features of the main approaches for computing gradients in DAE systems may be found in [35].

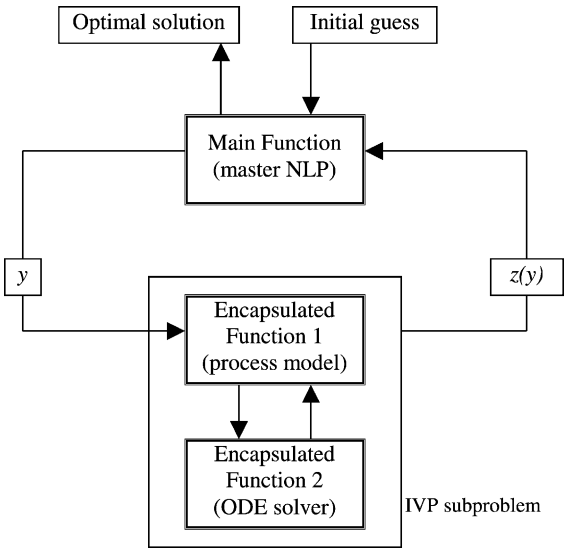

Fig. 4. Functional structure of the implemented sequential strategy.

However, the nylon-6,6 process model presented in Section 2 involves a complex mathematical dependence between the objective (as well as part of the constraints) and the control y, in such mode that analytical derivation of the gradients would be a hard task. This becomes an important drawback to the use of sensitivity approaches based on derivative evaluation. Therefore, sensitivities are not derived and the optimization is carried out through an SQP algorithm structured as shown in Fig. 4.

3.3. Simultaneous strategy

In the simultaneous strategy, the DAE solution and optimization converge simultaneously through the discretization of both state and control profiles. The ODEs are discretized using, for example, the A-stable orthogonal collocation on finite elements [25] and the resulting algebraic equations are added to the NLP formulation having the polynomial coefficients as optimization variables. Alternative approaches such as B-spline collocation can also be applied [24,36]. Consequently, the ODE model is solved only once over the optimization procedure. The main advantages of this approach lies on the treatment of profile constraints as well as bounds and elimination of costly and possibly infeasible intermediate solutions. Conversely, the major deficiency of this strategy lies in its explosive dimension. Neither this strategy nor the preceding one (Section 3.1) is ensured to be stable [37]. The stability issues for the simultaneous

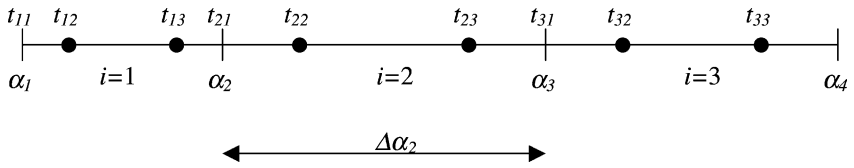

Fig. 5. Scheme of finite element collocation for $K = 2$ and NE = 3.

strategy are depicted in [37,38]. In addition, the formulation is characterized by a high degree of nonlinearity associated to the element placement constraints. As a result, the procedure can be very sensitive to starting points and must require a careful initialization [16,19].

In this paper, we are concerned with the orthogonal collocation method, which is as follows. To convert the DAOP defined in (4) into a nonlinear program we first discretize the ODEs by applying orthogonal collocation on finite elements [25]. Consider Fig. 5, where three finite elements (NE = 3) and two inner collocation points ($K = 2$) are represented. The location of the collocation points are chosen to correspond to the shifted roots of an orthogonal Legendre polynomial of degree K. The time domain $t \in [0, t_f]$ is normalized and partitioned into NE finite elements, where element i is bounded by two knots, α_i and α_{i+1}, with $\Delta\alpha_i = \alpha_{i+1}–\alpha_i$, $i = 1, \ldots, \text{NE}$, where clearly $\alpha_0 = 0$ and $\alpha_{\text{NE}+1} = 1$. By mapping each finite element to normalized time, say $\mathtt{t} \in [0, 1]$, the relationship between t and $\mathtt{t}$ becomes as follows:

$$t = \alpha_i + \mathtt{t}(\alpha_{i+1} - \alpha_i), \quad i = 1, \ldots, \text{NE}$$
$$\text{for} \quad t \in [\alpha_i, \alpha_{i+1}] \tag{6}$$

and the locations of the orthogonal Legendre roots in each element i are mapped to the following points:

$$t_{ij} = \alpha_i + \mathtt{t}_j(\alpha_{i+1} - \alpha_i),$$
$$i = 1, \ldots, \text{NE}, \ j = 0, \ldots, K \tag{7}$$

where $\mathtt{t}_j$ is the relative, normalized location of the jth ($j > 0$) shifted root of an orthogonal Legendre polynomial of degree K. Also, $\mathtt{t}_0 = 0$ is imposed to ensure the existence of a coefficient at the beginning of each element. State and control variable profiles, $Z(t)$ and $U(t)$ are approximated over each element i by Lagrange interpolation polynomials, respectively:

$$z^i_{K+1}(t) = \sum_{j=0}^{K} z_{ij}\varphi_{ij}(t), \qquad \varphi_{ij}(t) = \prod_{k=0,j}^{K} \frac{t - t_{ik}}{t_{ij} - t_{ik}} \tag{8}$$

$$u^i_K(t) = \sum_{j=1}^{K} \mathsf{u}_{ij}\psi_{ij}(t), \quad \psi_{ij}(t) = \prod_{k=1,j}^{K} \frac{t - t_{ik}}{t_{ij} - t_{ik}} \tag{9}$$

where $k = 0$, j denotes $k = 0, \ldots, j–1, j + 1, \ldots, K$. The term $z^i_{K+1}(t)$ denotes a $(K + 1)$th order (degree $< K + 1$) polynomial whereas $u^i_K(t)$ denotes a Kth order (degree $< K$) polynomial. The difference in the orders is due to the initial condition for $Z(t)$. Note that $z^i_{K+1}(t_{ij}) = \mathsf{z}_{ij}$ and $u^i_K(t_{ij}) = \mathsf{u}_{ij}$. As pointed out in [25], this property of the Lagrange polynomials is very desirable, since for chemical engineering problems states and controls often represent physical quantities, such as temperature or concentration. This in turn becomes useful when providing bounds on variables, initializing a profile or interpreting solution profiles. Replacing Eqs. (8) and (9) into the ODE model and enforcing the ODE in each element at the K shifted roots (t_{il}) of a Kth degree Legendre polynomial leads to the following collocation (or residual) equations:

$$R(t_{il}, \Delta\alpha_i) = \sum_{j=0}^{K} \mathsf{z}_{ij}\dot{\varphi}_{ij}(t_{il}) - F[x, \mathsf{u}_{il}, \mathsf{z}_{il}, t_{il}] = 0,$$
$$i = 1, \ldots, \text{NE}, \ l = 1, \ldots, K \tag{10}$$

with $z_{10} = Z_0$.

The calculation of $\dot{\varphi}_{ij}(t_{il})$ can be simplified [25] and Eq. (10) is rewritten as:

$$R(t_{il}) = \sum_{j=0}^{K} \mathsf{z}_{ij} \frac{\dot{\varphi}_j(t_l)}{\Delta\alpha_i} - F[x, \mathsf{u}_{il}, \mathsf{z}_{il}, t_{il}] = 0,$$
$$i = 1, \ldots, \text{NE}, \ l = 1, \ldots, K \tag{11}$$

with $z_{10} = Z_0$.

The expression for $\dot{\varphi}_j(t_l)$ can be easily calculated off-line through the following recursive formula:

$$\dot{\varphi}_j(t_l) = \left(\frac{2t_l - \sum_{j'=0,j}^{K} t_j}{t_j^2 - t_j \sum_{j'=0,j}^{K}(t_j) + \prod_{j'=0,j}^{K}(t_j)} \right),$$
$$j = 0, \ldots, K, \ l = 1, \ldots, K \tag{12}$$

An additional set of equations enforces continuity for $z^i_{K+1}(t)$ at the interior knots α_i, $i = 1, \ldots, \text{NE}$, as follows:

$$\mathsf{z}_{i0} = \sum_{j=0}^{K} \mathsf{z}_{i-1,j}\varphi_j(t = 1), \quad i = 2, \ldots, \text{NE},$$
$$\varphi_j(t) = \prod_{k=0,j}^{K} \frac{t - t_k}{t_j - t_k} \tag{13}$$

These equations extrapolate the polynomial $z^{i-1}_{K+1}(t)$ to the end point of its element and provide an initial condition for the next polynomial $z^i_{K+1}(t)$. Although differentiable and piecewise polynomial approximations for the state profile

can also be used, the continuous and piecewise approximation described in this section is sufficient in the present work, particularly since the process model may have nondifferentiable solution profiles. Therefore, the following NLP formulation is obtained:

$$\begin{aligned}
&\underset{x,u_{il},z_{il}}{\text{Min}} && \varphi[x, u_{il}, z_{il}] \\
&\text{s.t.} && c[x, u_{il}, z_{il}] = 0, \quad R(t_{i,l}) = 0, \\
& && i = 1, \ldots, \text{NE}, \ l = 1, \ldots, K, \\
& && z_{10} = Z_0, \quad z_{i0} = \sum_{j=0}^{K} z_{i-1j}\varphi_j \ (t = 1), \\
& && i = 2, \ldots, \text{NE}, \quad x^{\text{L}} \le x \le x^{\text{U}}, \\
& && U^{\text{L}} \le u_{il} \le U^{\text{U}}, \quad Z^{\text{L}} \le z_{il} \le Z^{\text{U}}
\end{aligned} \tag{14}$$

So far, the accuracy of the approximation however has not been discussed. Choosing a number of elements so that their lengths are "sufficiently small" is the first idea to minimize the approximation error. Indeed, an appropriate placement of these elements has a severe impact on this number and in fact is the procedure to be followed, as discussed in the next section.

3.3.1. Incorporating knot placement in optimization

Numerous strategies exist in the approximation theory literature for selecting a suitable distribution of knots when finite elements are used. Russell and Christiansen [39] present an excellent review where numerical comparisons are included. Cuthrell and Biegler [25] develop a nonfully rigorous method based on error equidistribution, in which the introduction of nondifferentiabilities and highly nonlinear equations can be regarded as major deficiencies. This work is extended by Cuthrell and Biegler [38] for discontinuous control and refined by Vasantharajan and Biegler [27] by developing a more reliable strategy where the approximation error can be controlled directly in parameter optimization. Extension to optimal control problems is explored by Logsdon and Biegler [26] where many of the previous concepts can be applied. The major distinction is that optimality conditions for optimal control problems are systems of DAEs and for certain conditions, as saturation of state variable profiles, stability and accuracy problems can occur, which is not encountered with parameter optimization problems [27].

In order to control the overall error within every element for all of the differential equations in the simultaneous approach, we consider [37], which is based on the enforcement of the following constraints in the optimization formulation:

$$r^i = \frac{1}{2}\sum_{m=1}^{M}(R(t_{nc}^i)_m^2 \Delta\alpha_i) \le \varepsilon, \quad i = 1, \ldots, \text{NE} \tag{15}$$

where $R(t_{nc}^i)_m$ denotes the residual at the noncollocation point t_{nc} of the mth state profile at the finite element i and ε is a user-specified error tolerance. The residuals $R(t_{nc}^i)_m$ can be calculated through Eq. (11) by extrapolating the states and controls at t_{nc} with Eqs. (8) and (9). Therefore, the resulting optimization problem is as follows [37]:

$$\begin{aligned}
&\underset{x,u_{il},z_{il}}{\text{Min}} && \phi[x, \mathsf{u}_{il}, \mathsf{z}_{il}] \\
&\text{s.t.} && c[x, \mathsf{u}_{il}, \mathsf{z}_{il}] = 0, \quad R(t_{i,l}, \Delta\alpha_i) = 0, \\
& && i = 1, \ldots, \text{NE}, \ l = 1, \ldots, K, \\
& && \mathsf{z}_{10} = Z_0, \quad \mathsf{z}_{i0} = \sum_{j=0}^{K} \mathsf{z}_{i-1j}\varphi_j \ (\mathrm{t} = 1), \\
& && i = 2, \ldots, \text{NE}, \\
& && \frac{1}{2}\sum_{m=1}^{M}(R(t_{nc}^i)_m^2 \Delta\alpha_i) \le \varepsilon, \\
& && i = 1, \ldots, \text{NE}, \quad \Delta\alpha_i \ge 0, \quad i = 1, \ldots, \text{NE}, \\
& && \sum_{i=1}^{\text{NE}} \Delta\alpha_i = t_f, \quad x^{\text{L}} \le x \le x^{\text{U}}, \\
& && U^{\text{L}} \le \mathsf{u}_{il} \le U^{\text{U}}, \quad Z^{\text{L}} \le \mathsf{z}_{il} \le Z^{\text{U}}
\end{aligned} \tag{16}$$

As pointed out in [37], this enforcement is only effective for index 1 problems, since for higher index systems the accuracy of the higher index variables is affected due to reduction of the error order. In these cases, a different error control strategy on higher index variables (usually the controls) is required. Furthermore, from theoretical properties developed by Brenan and Petzold [40], high index systems (i.e., index 2 or higher) can be considered not only by controlling the integration error, but by additionally choosing a suitable method. The minimum requirements for these methods are [37]: index 1 problems, two-point collocation; index 2 problems, three-point collocation; index 3 problems, four-point collocation.

The integral terms in Tables 4 and 6 may be properly removed by adding an extra state and a corresponding differential equation. The fundamental nylon-6,6 process model is rewritten as in (17) and Table 7, which is an index 1 DAE

Table 7
Functions of (17)

Kinetics: $R_1' = k_1 c$; $R_2' = l\left(k_2 + k_3\left(\frac{a}{\tau}\right)\right)$; $R_3' = \left(\frac{k_{\text{app}}}{\tau}\right)\left(ac - \left(\frac{lw}{K_{\text{app}}}\right)\right)$
$k_i = f(T)$, $i = 1, 2, 3$; $K_{\text{app}} = f(T, w, \tau)$; $K_0 = f(w, \tau)$; $k_{\text{app}} = f(T)$; $k_0 = f(w, c, \tau)$
$\Delta H_{\text{app}} = f(w, \tau)$; $\Delta H_{\text{v}}^{\text{w}} = f(T)$; $C_p = f(T, c, \text{se}, a, \varpi, w, \theta)$
Mass transfer model: v, $v_i^{\text{M}} = f(P, T, l, w, \text{hmd}, \tau)$, $i = \text{A}, \text{W}, \text{HMD}$; $\omega_{\text{HMD}}^{\text{e}} = f(T, w, \text{hmd}, \tau)$, where $\tau = f(a, c, l, w, \text{se})$ and $\text{hmd} = f(a, c, \text{se}, \varpi)$

because one differentiation step is needed to obtain an expression for P and Q_{heat} from active bounds:

$$
\begin{aligned}
\max_{P,Q_{\text{heat}}} \quad & l(t_f) \\
\text{s.t.} \quad & \frac{\mathrm{d}a}{\mathrm{d}t} = R_2' - (R_3' + v_{\text{A}}^{\text{M}}), \quad \frac{\mathrm{d}c}{\mathrm{d}t} = -(R_3' + R_1'), \\
& \frac{\mathrm{d}l}{\mathrm{d}t} = R_3' - R_2', \quad \frac{\mathrm{d}w}{\mathrm{d}t} = R_3' + R_1' - v_{\text{w}}^{\text{M}}, \\
& \frac{\mathrm{d}\,\text{se}}{\mathrm{d}t} = R_1' + R_2' \, \frac{\mathrm{d}\theta}{\mathrm{d}t} = -v, \\
& \frac{\mathrm{d}T}{\mathrm{d}t} = -\frac{\Delta H_{\text{app}} R_3'}{\theta C_p} - \frac{\Delta H_{\text{v}}^{\text{HMD}} v_{\text{HMD}}^{\text{M}}}{\theta C_p} \\
& \qquad -\frac{\Delta H_{\text{v}}^{\text{W}} v_{\text{W}}^{\text{M}}}{\theta C_p} + \frac{Q_{\text{heat}}}{\theta C_p}, \\
& \frac{\mathrm{d}\varpi}{\mathrm{d}t} = \frac{2\omega_{\text{HMD}}^{\text{e}} v}{M_{\text{HMD}}}, \quad \text{MW} = f(c, \text{se}, a, \varpi), \\
& \text{NH}_2 = f(a, \theta)
\end{aligned}
\tag{17}
$$

where R_i' $(i = 1, 2, 3)$ are defined as:

$$R_1' = k_1 c, \qquad R_2' = l\left(k_2 + k_3\left(\frac{a}{\tau}\right)\right),$$

$$R_3' = \left(\frac{k_{\text{app}}}{\tau}\right)\left(ac - \left(\frac{lw}{K_{\text{app}}}\right)\right)$$

and, as Tables 2–6:

$$k_i = f(T), \quad i = 1, 2, 3, \quad K_{\text{app}} = f(T, w, \tau),$$
$$K_0 = f(w, \tau), \quad v, v_i^{\text{M}} = f(P, T, l, w, \text{hmd}, \tau),$$
$$i = \text{A}, \text{W}, \text{HMD}, \quad \Delta H_{\text{app}} = f(w, \tau), k_{\text{app}} = f(T),$$
$$k_0 = f(w, c, \tau), \quad \Delta H_{\text{v}}^{\text{w}} = f(T),$$
$$C_p = f(T, c, \text{se}, a, \varpi, w, \theta)e, \quad \omega_{\text{HMD}}^{\text{e}} = f(T, w, \text{hmd}, \tau)$$

where $\tau = f(a, c, l, w, \text{se})$ and $hmd = f(a, c, \text{se}, \varpi)$.

Table 8
Initial conditions for the nylon-6,6 problem

State variable	Initial value
$C_{\text{A}0}$ (mol/l)	6
$C_{\text{C}0}$ (mol/l)	6
$C_{\text{L}0}$ (mol/l)	0
$C_{\text{W}0}$ (mol/l)	11.2
$C_{\text{SE}0}$ (mol/l)	0
ρ_0 (kg/l)	0.971
V_0 (l)	1802
T_0 (K)	425

In (17), the lower case letters denote the product of volume and concentration; for instance, $a = C_{\text{A}} V$ and so on. Model (17) has as initial condition $\varpi(0) = 0$, since the amount of vaporized HMD is zero at the beginning of the batch. If necessary, the volume of liquid phase can be computed by incorporating the algebraic constraint $V = \theta\, \hat{V}_{\text{sol}}$, where $\hat{V}_{\text{sol}} = f(T, w, l, \theta)$. Note that constraints on nylon-6,6 qualities must only be active at one point of the trajectory $(t = t_f)$. This allows two-point collocation to find the solution because the higher index portion does not propagate into the index 1 portion of the system.

4. Results

4.1. Model simulation

In order to provide an accurate starting point for the simultaneous strategy, the process model (Tables 2–6) was firstly simulated by using typical operational values as estimates for the input heat and reactor pressure profiles. The model simulation for a horizon of 3 h for typical initial conditions summarized in Table 8 was accomplished by MATLAB® on a Pentium III 700 MHz platform in 0.77 CPUs. Figs. 6 and 7

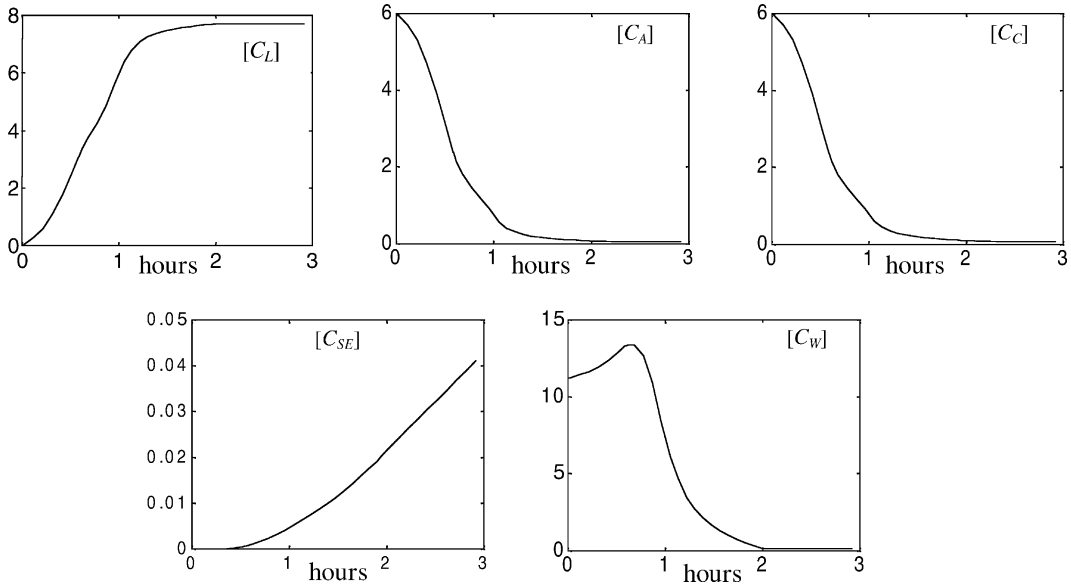

Fig. 6. Typical simulation results for concentration of functional groups during a batch run.

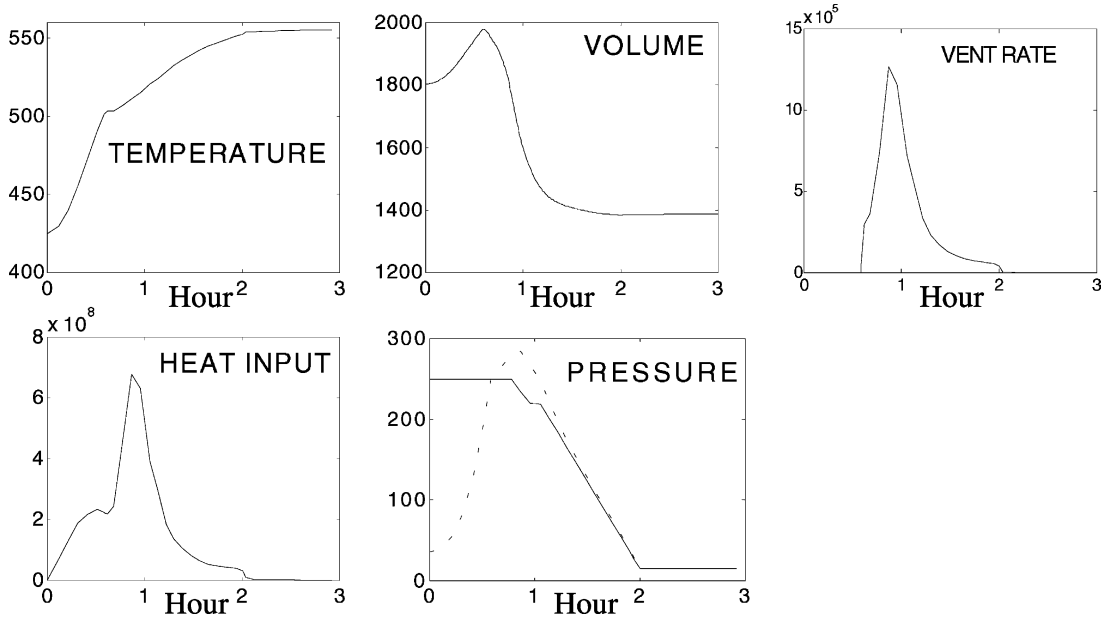

Fig. 7. Typical simulation results for the autoclave model parameters during a batch run and initial estimate for the heat input, reactor (solid line) and vapor (dashed line) pressures.

display typical simulated trajectories for the key process variables. The initial guesses for the input heat and reactor pressure profiles are also presented in Fig. 7.

4.2. Model optimization

In order to start the optimization procedure, both strategies make use of the same initial estimate for heat input and reactor pressure profiles are shown in Fig. 7. As mentioned in the preceding section, the simultaneous strategy also relies on the simulated response as initial point for the NLP solver. Moreover, two models are sequentially solved within the simultaneous approach. In the first one, the time-invariant model, an evenly spaced set of fixed knots are used to discretize the horizon. Based on the previous results, the optimization of Eq. (16) is then accomplished by relaxing the aforementioned knot placement constraint. Without this procedure, expensive computation and frequent failures were encountered during the optimization.

The objective is to maximize the production of the desired polymer satisfying product specifications ($MW^{target} = 13\,479$ and $NH_2^{target} = 49.7$) for a nominal batch run time of 3 h. The sequential strategy employs a piecewise linear control policy under 30 sampling intervals of the same length, with the requirement for continuity of the control from one finite element to another. The coefficients of (5) were chosen as $\gamma = 1.5$, $\eta = 0.5$ and $\omega = 7 \times 10^{-5}$. The SQP approach is used to implement the feasible path optimization in MATLAB®. Here, the resulting quadratic program determines the search direction whereas a line search procedure along the direction defines the next point. On the other hand, the GRG-based solver CONOPT2 [41] accomplishes the simultaneous based optimization. Here, discontinuities introduced by *max* operators (Table 5) may be easily eliminated through smooth approximation techniques. The modeling system GAMS 2.50 [42] was used in order to implement the model and its solution method. The choice for the number of finite elements used to discretize (16) was supported by comparisons between simulated and optimized profiles. For two collocation points ($K = 2$), 10 finite elements (NE = 10) have proven to be sufficient for obtaining satisfactory profile approximations ($\varepsilon = \varepsilon_r = 10^{-3}$) within acceptable computational effort.

The results of the simultaneous optimization are given in Table 9 where computational details, including the model dimension and CPU times are also tabulated. Table 10 reports

Table 9
Simultaneous approach performance and related information ($\varepsilon = \varepsilon_r = 10^{-3}$)

Number of constraints	Number of variables	Number of iterations	CPU time (s)	Objective = max $[C_L]$ (mol/l)
Evenly spaced knots based model				
1327	1379	451	20.33	7.722
Direct error enforcement based model				
1760	1639	430	38.16	7.722

Table 10
Initial and optimal knot distribution (simultaneous approach)

	α_i, $i = 1, \ldots, \mathrm{NE}+1$										
Initial	0	0.3	0.6	0.9	1.2	1.5	1.8	2.1	2.4	2.7	3.0
Final	0	0.323	0.57	0.71	1.03	1.17	1.699	1.839	2.72	2.86	3.0

Table 11
Summary of the results

Solution strategy	Objective = max [CL] (mol/l)	MW quality (target: 13479)	NH_2 quality (target: 49.7)	Total CPU time (s)
Sequential	7.992	13479	46.13	133
Simultaneous	7.722	13490	50.20	58.8
Initial estimate	7.687	10918	64.50	0.77

the initial (uniform) and optimal knot distribution. Objective values and resulting product qualities are summarized in Table 11. The resulting profiles for key variables are compared in Fig. 8. The reliability of the approximation may be checked by comparing the final collocation profiles with those obtained by numerical integration, as shown in Fig. 9. Finally, in Fig. 10 the heat input and reactor pressure optimal profiles produced by the two strategies as well as the initial estimate are compared. Here, note that how the heat input peak provided by the simultaneous solution shifts in size and position from the sequential one as result of the existence of multiple (local) optimal solutions.

After 133 iterations there were no significant improvements in the objective value and the sequential procedure has stopped at this point. However, this feasible approach is more time-consuming than the simultaneous one since it requires repeated and expensive solution of the overall DAE system (Table 11). Furthermore, computational cost is still high due to the need of parallel convergence of the quality parameters in (4), since the state variable bounds cannot be enforced in a straightforward way. Nevertheless, the computational performance of the proposed sequential approach can be acceptable for industrial purposes.

Table 9 summarizes model features and related computational performance of the simultaneous strategy. As can be seen, although substantially larger, the variable-knot model was solved in a smaller number of iterations, which were clearly more time-consuming tasks than the previous ones. Apparently, this results from its starting point (note that the objective value remains the same), which is the solution of the fixed knot model. Despite appreciable changes in the knot distribution (Table 10), particularly in the final instants of the horizon (product depuration), no improvement was verified for the objective value. However, this is not surprising since the second model (variable-knot location), albeit less constrained than the first model (fixed knot location)

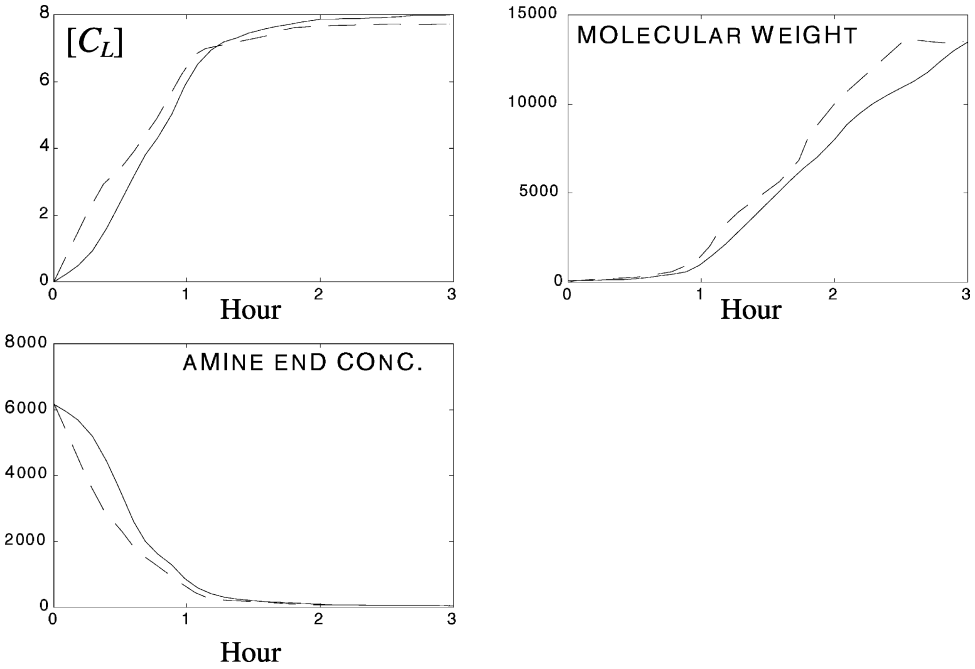

Fig. 8. Optimal profiles for key variables obtained with sequential (solid line) and simultaneous (dashed line) approaches.

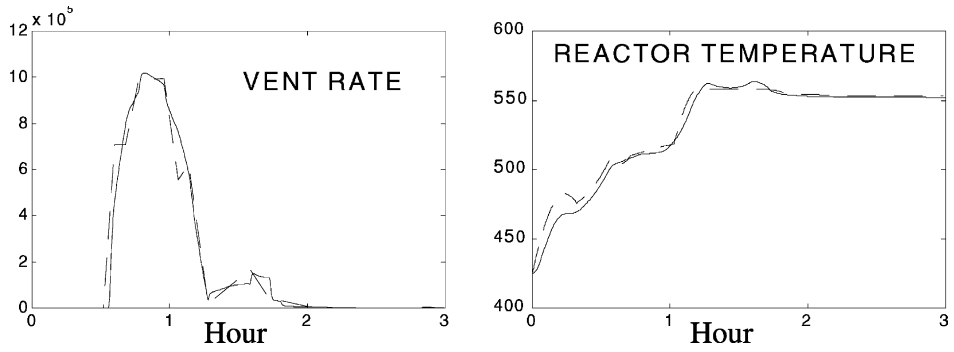

Fig. 9. Optimal profiles obtained through collocation (dashed) and the correspondent ones produced by numerical integration (solid line) of the solution.

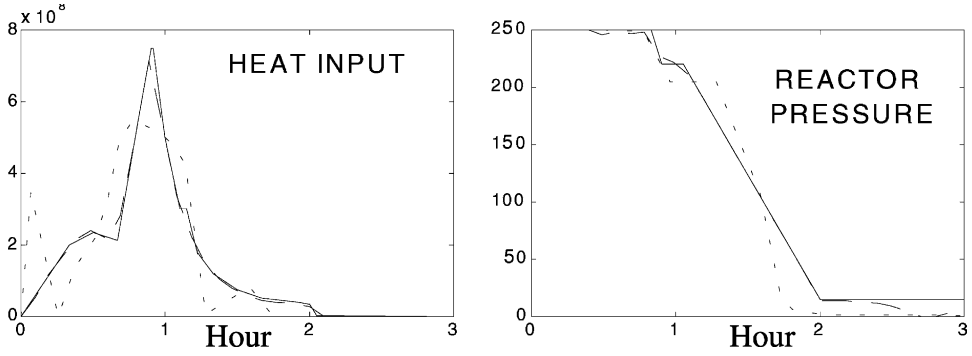

Fig. 10. Optimal profiles obtained through the sequential (long dashed) and simultaneous (short dashed) approaches and the initial estimate (solid line) for the controls.

from the knot placement viewpoint is more restricted in what concerns the approximation error. As a consequence, comparative worst objective were not rare when running the second formulation. Finally, Table 11 demonstrates the effectiveness of both optimization strategies over the simulated results provided by the initial estimate for the control profiles.

5. Concluding remarks

In this contribution the dynamic optimization problem of batch nylon-6,6 autoclave process has been presented and solved through NLP techniques in order to evaluate their capabilities for determining optimal operating profiles. As a basis for the proposed study, the process model from Russell et al. [9] was chosen due to the its suitable and well-known phenomenological structure. A qualitative dynamic optimization that takes into account operation conditions, wear and tear of the equipment, product quality and energy consumption is then accomplished through two distinct NLP-based solution strategies.

Several concepts were discussed in order to introduce the necessary background for the proposed study. First, we took an in-depth view of the batch nylon-6,6 autoclave process and introduced the fundamental process model. Inherent features of the sequential and simultaneous methods were then discussed and formalized. A simpler and reliable strategy from [37] where the approximation error can be controlled was also outlined and implemented within the simultaneous approach. In particular, regarding the well-known difficulties in finding global solutions for large-scale nonconvex NLP models, this study is concerned with local optima determination.

Beyond the aforementioned dimension and nonconvexity issues, the nylon-6,6 batch autoclave model is characterized by its large diversity in size order of the variable set (values ranging from $\sim 10^{-5}$ to 10^{9}). Therefore, it is mandatory to perform good variable and equation scaling or meaningless solutions can be reported with the simultaneous approach. In counterpart, a suitable selection of the error term coefficients as well as the scaling of the controls is imperative to accomplish the optimization in competitive CPU times through the sequential strategy. As a consequence, the improved performance of both strategies is usually achieved only after an expressive level of investment in terms of modeling implementation. Results have shown that both strategies can be successfully applied to solve the nylon-6,6 batch autoclave optimization problem. Nevertheless, the simultaneous strategy enables that quality constraints on state variables are imposed in a straightforward manner and therefore generates better and more robust solutions.

Acknowledgements

This work was financially supported by FAPESP grants 98/14384-3 and 99/09897-4.

References

[1] J.M. Pinto, M. Joly, L.F.L. Moro, Planning and scheduling models for refinery operations, Comput. Chem. Eng. 24 (2000) 2259–2276.
[2] N. Ogata, Studies on polycondensation reactions of nylon salt. I. The equilibrium in the system of polyhexamethylene adipamine and water, Macromol. Chem. 42 (1960) 52–67.
[3] N. Ogata, Studies on polycondensation reactions of nylon salt. II. The rate of polycondensation reaction of nylon-6,6 salt in the presence of water, Macromol. Chem. 43 (1961) 117–131.
[4] D.D. Steppan, M.F. Doherty, M.F. Malone, A kinetic and equilibrium model for nylon-6,6 polymerization, J. Appl. Polym. Sci. 33 (1987) 2333–2344.
[5] L. Jacobsen, W.H. Ray, Unified modeling for polycondensation kinetics, J. Macromol. Sci.-Rev. Macromol. Chem. Phys. C32 (3–4) (1992) 407–519.
[6] D.D. Steppan, M.F. Doherty, M.F. Malone, Wiped film reactor model for nylon-6,6 polymerization, Ind. Eng. Chem. Res. 29 (1990) 2012–2020.
[7] B.R. Choi, H.H. Lee, Transient and steady-state behavior of wiped-film reactors for reversible condensation polymerization, Ind. Eng. Chem. Res. 35 (5) (1996) 1550–1555.
[8] R. Giudici, C.A.O. Nascimento, I.C. Beiler, N. Scherbakoff, Modeling of industrial nylon-6,6 polycondensation process in a twin-screw extruder reactor. I. Phenomenological model and parameter adjusting, J. Appl. Polym. Sci. 67 (1998) 1573–1587.
[9] S.A. Russell, D.G. Robertson, J.H. Lee, B.A. Ogunnaike, Control of product quality for batch nylon-6,6 autoclaves, Chem. Eng. Sci. 33 (21) (1998) 3685–3702.
[10] T. Yabuki, T. Nagasawa, J.F. MacGregor, Industrial experiences with product quality control in semi-batch processes, Comput. Chem. Eng. 26 (2002) 205–212.
[11] T. Clarke-Pringle, J.F. MacGregor, Nonlinear adaptive temperature control of multi-product, semi-batch polymerization reactors, Comput. Chem. Eng. 21 (12) (1997) 1395–1409.
[12] R. Giudici, C.A.O. Nascimento, A. Tresmondi, A. Domingues, R. Pellicciotta, Mathematical modeling of an industrial process of nylon-6,6 polymerization in a two-phase flow tubular reactor, Chem. Eng. Sci. 54 (1999) 3243–3249.
[13] C.A.O. Nascimento, R. Giudici, R. Guardani, Neural network based approach for optimization of industrial chemical processes, Comput. Chem. Eng. 24 (2000) 2303–2314.
[14] C. Duchesne, J.F. MacGregor, Multivariate analysis and optimization of process variable trajectories for batch processes, Chemomet. Int. Lab. Syst. 51 (2000) 125–137.
[15] W.F. Feehery, P.I. Barton, Dynamic optimization with equality path constraints, Ind. Eng. Chem. Res. 38 (1999) 2350–2363.
[16] P. Tanartkit, L.T. Biegler, Stable decomposition for dynamic optimization, Ind. Eng. Chem. Res. 34 (1995) 1253–1266.
[17] M. Amon, C.D. Denson, Simplified analysis of the performance of wiped-film polycondensation reactors, Ind. Eng. Chem. Fundam. 19 (1980) 415–421.
[18] P.J. Flory, Molecular size distribution in linear condensation polymers, J. Am. Chem. Soc. 58 (1936) 1877–1885.
[19] W.F. Feehery, P.I. Barton, Dynamic optimization with state variable path constraints, Comput. Chem. Eng. 22 (9) (1998) 1241–1256.
[20] R. Bellman, Dynamic Programming, Princeton University Press, Princeton, NJ, 1957.
[21] R. Luus, Application of dynamic programming to high-dimensional nonlinear optimal control problems, Int. J. Control 52 (1990) 239–250.
[22] L.S. Pontryagin, V.G. Boltyanskii, R.V. Gamkrelidze, E.F. Mishchenko, The Mathematical Theory of Optimal Processes, Interscience, New York, 1962.
[23] R.W.H. Sargent, G.R. Sullivan, The development of an efficient optimal control package, in: Proceedings of the Eighth IFIP Conference on Optim. Tech., Part 2, 1977.
[24] C.P. Neuman, A. Sen, A suboptimal control algorithm for constrained problems using cubic splines, Automatica 9 (1973) 601–603.
[25] J.E. Cuthrell, L.T. Biegler, On the optimization of differential-algebraic process systems, AIChE J. 33 (8) (1987) 1257–1270.
[26] J.S. Logsdon, L.T. Biegler, Decomposition strategies for large scale dynamic optimization problems, Chem. Eng. Sci. 47 (4) (1992) 851–862.
[27] S. Vasantharajan, L.T. Biegler, Simultaneous strategies for optimization of differential-algebraic systems with enforcement of error criteria, Comput. Chem. Eng. 14 (10) (1990) 1083–1100.
[28] W.F. Feehery, P.I. Barton, Dynamic simulation and optimization with inequality path constraints, Comput. Chem. Eng. 20 (1996) S707–S712.
[29] V.S. Vassiliadis, R.W.H. Sargent, C.C. Pantelides, Solution of a class of multistage dynamic optimization problems. Part II. Problems with path constraints, Ind. Eng. Chem. Res. 33 (1994) 2123–2133.
[30] P. Wolfe, The Reduced Gradient Method, RAND Co., 1962.
[31] S.P. Han, Superlinearly convergent variable metric algorithms for general nonlinear programming problems, Math. Prog. 11 (1976) 263–282.
[32] J. Banga, W. Seider, Global optimization of chemical processes using stochastic algorithms, in: State of the Art in Global Optimization: Computational Methods and Applications, Princeton University Press, Princeton, NJ, 1995.
[33] E.F. Carrasco, J.R. Banga, Dynamic optimization of batch reactors using adaptive stochastic algorithms, Ind. Eng. Chem. Res. 36 (1997) 2252–2261.
[34] O. Rosen, R. Luus, Evaluation of gradients for piecewise constant optimal control, Comput. Chem. Eng. 15 (4) (1991) 273–281.
[35] V.S. Vassiliadis, R.W.H. Sargent, C.C. Pantelides, Solution of a class of multistage dynamic optimization problems. Part I. Problems without path constraints, Ind. Eng. Chem. Res. 33 (1994) 2111–2122.
[36] T. Binder, L. Blank, W. Dahmen, W. Marquardt, Grid refinement in multiscale dynamic optimization, in: S. Pierucci (Ed.), ESCAPE 10, Elsevier, Amsterdam, 2000, pp. 31–36.
[37] J.S. Logsdon, L.T. Biegler, Accurate solution of differential-algebraic optimization problems, Ind. Eng. Chem. Res. 28 (1989) 1628–1639.
[38] J.E. Cuthrell, L.T. Biegler, Simultaneous optimization and solution methods for batch reactor control profiles, Comput. Chem. Eng. 13 (1989) 49–62.
[39] R.D. Russell, J. Christiansen, Adaptive mesh selection strategies for solving boundary-value problems, SIAM J. Num. Anal. 15 (1) (1978) 59–80.
[40] K.E. Brenan, L.R. Petzold, The numerical solution of higher index differential/algebraic equations by implicit Runge–Kutta methods, UCRL Preprint 95905, Lawrence Livermore National Laboratories, Livermore, CA, 1986.
[41] A.S. Drud, A system for large scale nonlinear optimization, Reference Manual for CONOPT Subroutine Library, ARKI Consulting and Development A/S, Bagsvaerd, Denmark, 1996.
[42] A. Brooke, D. Kendrick, A. Meeraus, R. Raman, GAMS—A User's Guide, The Scientific Press, Redwood City, CA, 1998.